# Stability and bifurcations in time-delay systems: A novel and efficient blend of methods

# GRISELDA R. ITOVICH\*

Escuela de Producción, Tecnología y Medio Ambiente, Sede Alto Valle y Valle Medio, Universidad Nacional de Río Negro R8336ATG Villa Regina, Argentina

### FRANCO S. GENTILE

Departamento de Matemática, Universidad Nacional del Sur Instituto de Investigaciones en Ingeniería Eléctrica - IIIE (UNS - CONICET) B8000CPB Bahía Blanca, Argentina

### JORGE L. MOIOLA

Departamento de Ingeniería Eléctrica y de Computadoras, Universidad Nacional del Sur Instituto de Investigaciones en Ingeniería Eléctrica - IIIE (UNS - CONICET) B8000CPB Bahía Blanca, Argentina

Received (to be inserted by publisher)

The goal of this article is to introduce a hybrid technique, combining two existing methods conveniently, to analyze stability and bifurcations of equilibrium points and periodic orbits in delay-differential equations of retarded type. One method is called the frequency-domain approach, an analytical tool based on control theory allowing to detect and represent periodic solutions emerging from Hopf bifurcations, via Fourier series and harmonic balances. The second one, the so-called semi-discretization method, provides a numerical scheme to approximate the monodromy operator of a periodic solution, thus permitting to establish stability and bifurcations of limit cycles as well as analyzing equilibrium points. It is shown that a proper combination of these methods provides a straightforward strategy to study both local and global bifurcations in time-delay systems. The usefulness of the proposed approach is shown by three examples, where the results are compared with those given by the software Dde-Biftool.

Keywords: Semi-discretization, frequency-domain approach, time-delay system, bifurcation, limit cycle

### 1. Introduction

In the usual framework of control systems, timedelays have negative effects. They can cause loss of stability, simple or multiple oscillations, and more complex dynamics. Those behaviours are commonly avoided in practical situations by the implementation of sufficiently fast controllers. However, in applications where the system dynamics is rapid compared with the control response, and time-delays cannot be neglected, the mathematical treatment of the resulting model is challenging. On the other hand, there are special control schemes which rely

<sup>\*</sup>E-mail: gitovich@unrn.edu.ar

on the intentional occurrence of a time-delay, for example in Pyragas control [Pyragas, 1992]. Concerning the equilibrium points stability, as the number of eigenvalues of the linearized system is infinite, the system is prone to suffer instabilities when one or more parameters vary. Another difficulty lies on detecting the appearance of oscillatory phenomena. In this direction, it is possible to track of Tsypkin's pioneer contributions [Tsypkin, 1946] using the Nyquist stability criterion.

There is a methodology to detect the appearance of a smooth oscillation when a bifurcation parameter is varied, based on the theory of feedback control [Mees, 1981]. This approach relies on the Graphical Hopf Bifurcation Theorem (GHBT), which is an alternative to the classical Hopf bifurcation theorem. The GHBT was developed for ordinary differential equations (ODEs) in the first instance [Mees & Chua, 1979; Mees, 1981], and then it was extended to delay-differential equations (DDEs) in [Moiola & Chen, 1996] and mainly in [Gentile et al., 2019].

As mentioned previously, some control schemes have been designed using delayed versions of the state variables, for example, to control chaotic dynamics [Pyragas, 1992; Nakajima, 1997]. Those techniques have an enormous advantage, this is, the experimental realization is very simple, and they do not require a precise model of the system. Moreover, the stabilization of the erratic dynamics into a periodic orbit immediately follows after a correct tuning of the delay parameter. A canonical example is the Rössler oscillator, in which the chaotic behaviour can be controlled using a simple feedback of delayed variables [Balanov et al., 2005]. In addition, some systems become stable when several signals with different time-delays are fed back [Kharitonov et al., 2005].

Thus, time-delays contribute to stabilize or destabilize the system, according to the specific application. They can modify the stability of equilibrium points (as usual in classical control systems) but also the properties of periodic orbits, for example, when an oscillation of a specific amplitude and frequency is desired. In the latter case, the stability of the periodic solution is difficult to be determined analytically, since the monodromy operator is needed, which in turn requires the expression of the periodic solution itself. In this sense, a well known technique using Tchebyschev polynomials can be seen in [Butcher & Mann, 2009]. Considering the mentioned difficulties, the main idea of

this article is to combine two techniques to study the stability of limit cycles. One of them is the already mentioned GHBT in DDEs, which provides an approximate expression of the periodic solution, whose accuracy depends on the number of harmonics employed in its Fourier representation [Moiola & Chen, 1996; Gentile et al., 2019]. The second technique is called semi-discretization, which consist of considering a discrete time scale that only affects the delayed terms of the equation, and leaving the non-delayed variables in their original form Insperger & Stépán, 2011]. It will be shown that the combination of both approaches is very effective for the determination of the stability of the periodic orbits. The results will be illustrated via three examples, two of them correspond to systems where the Pyragas [Pyragas, 1992] control strategy is employed, and the third one is a modified van der Pol oscillator.

# 2. Stability of limit cycles and equilibrium solutions

It is considered the following nonlinear, delaydifferential equation of the retarded type

$$\dot{x}(t) = f(x(t), x(t-\tau); \mu), \tag{1}$$

where  $x \in \mathbb{R}^n$  is the vector of state variables,  $\dot{x} = dx/dt, \, \tau \in \mathbb{R}^+$  is the time-delay,  $\mu \in \mathbb{R}^p$  is a vector of parameters and  $f: \mathbb{R}^n \times \mathbb{R}^n \times \mathbb{R}^p \longrightarrow \mathbb{R}^n$  is a smooth nonlinear function. The focus is on detecting the qualitative changes in the structure of solutions of (1) as long as the delay  $\tau$  and the vector  $\mu$  are varied. The stability of a (non constant) periodic solution  $\tilde{x}(t)$  (that can also depend on  $\mu$ ) of (1) of period T can be established by means of the linear time periodic DDE

$$\dot{y}(t) = L_0(t, \mu)y(t) + L_1(t, \mu)y(t - \tau), \qquad (2)$$

where

$$L_0(t,\mu) = \frac{\partial f}{\partial x}\Big|_{x=\tilde{x}}, \quad L_1(t,\mu) = \frac{\partial f}{\partial x(t-\tau)}\Big|_{x=\tilde{x}}.$$
(3)

Notice that  $L_0$  and  $L_1$  in (2-3) are T-periodic matrices in the variable t. In the following  $\tau \leq T$  must be assumed. The evolution of an arbitrary initial condition  $x(t) = \varphi(t), t \in [-\tau, 0]$  under the equation (2) in the interval  $[T - \tau, T]$  (or in any interval of length T) must be observed.

On the other hand, the stability of an equilibrium  $x^*$  of (1) satisfying  $0 = f(x^*, x^*; \mu)$ , can be

also deduced from (2) but evaluating the expressions in (3) at the constant solution  $x^*$  instead of  $x = \tilde{x}(t)$ . In this case,  $L_0 = L_0(\mu)$  and  $L_1 = L_1(\mu)$ , i.e., they become matrices only dependent on  $\mu$ . The equilibrium point  $x^*$  is asymptotically stable if and only if the characteristic equation

$$\left| \lambda I_n - L_0(\mu) - L_1(\mu) e^{-\lambda \tau} \right| = 0, \tag{4}$$

has all its eigenvalues in the open left-half of the complex plane, where  $I_n$  denotes the  $n \times n$  identity matrix. A stability change takes place if a root of (4) crosses to the right-half plane (while others remain in the left-half), when  $\tau$  or other parameter is varied. If a pair of complex conjugate roots cross the imaginary axis, a periodic solution may appear via a Hopf bifurcation.

#### 3. The frequency-domain approach

Let us express (1) as a feedback system

$$\dot{x}(t) = A_0 x(t) + A_1 x(t - \tau) + B u(t), \tag{5a}$$

$$y(t) = -Cx(t), (5b)$$

$$u(t) = g(y(t), y(t - \tau); \mu) = g(Y; \mu),$$
 (5c)

where matrices  $A_0, A_1$  are of size  $n \times n$ , B is  $n \times p$ and C is  $m \times n$ , which can obviously depend on the parameter  $\mu$ . Equation (5a) is a linear system with input  $u = g(Y, \mu) \in \mathbb{R}^p$  defined through (5b-5c). Then, g is a feedback function that concentrates all the nonlinear terms and may depend on both delayed and non-delayed variables. On the other hand, after applying the Laplace transform, the linear part is represented by the transfer function

$$G^*(s) = \begin{bmatrix} G(s) \\ G(s)e^{-s\tau} \end{bmatrix},$$

with

$$G(s) = C \left[ sI_n - A_0 - A_1 e^{-s\tau} \right]^{-1} B,$$
 (6)

where the dependence of  $G^*$  on  $\tau$  and  $\mu$  is omitted for short. Notice that the output of this linear subsystem is  $Y = [y(t) \ y(t-\tau)] \in \mathbb{R}^{2m}$ . Formulation (5a-5c) is the most general scheme that can be thought for delayed equations of retarded type, in which the delayed terms appear in both linear and nonlinear subsystems. The appearance of matrix  $A_1$ can be avoided absorbing all the delayed terms in the nonlinear function g, as shown in [Gentile *et al.*, 2019. This setting becomes much simpler if the delayed terms affect only the nonlinearity  $(A_1 = 0)$ , they only appear as linear terms (thus, they do not

appear in the feedback, i.e.,  $g = g(y(t); \mu)$  or the non-linearity depends on delayed terms only (thus, the feedback only includes delayed versions of the variables, i.e.,  $g = g(y(t - \tau); \mu)$ .

The (possible) equilibrium points  $Y^*$  of (5a-5c) are the solutions of  $G^*(0)g(Y^*; \mu) = -Y^*$  and the stability of  $Y^*$  is studied via the generalized Nyquist criterion. Let

$$J = \begin{bmatrix} \frac{\partial g}{\partial y(t)} & \frac{\partial g}{\partial y(t-\tau)} \end{bmatrix} \Big|_{Y=Y^*},$$

then the characteristic equation in the frequency domain reads

$$|\lambda I_{2m} - G^*(s)J| = 0.$$

The eigenvalues  $\lambda_1, \lambda_2, ..., \lambda_{2m}$  of  $G^*(s)J$  (also known as characteristic functions) depend on the complex variable s as well as the parameter  $\mu$  and  $\tau$ . Let  $s = i\omega$ ,  $\omega \in \mathbb{R}$ , then for fixed values of  $\mu$  and  $\tau$ , the geometrical locus of each  $\lambda_j$  can be traced out in the complex plane. Now, allowing a parameter variation, a stability change in  $Y^*$  is produced when a distinguished eigenvalue  $\hat{\lambda}(s)$  equals -1 for some  $s = i\omega_0$  with  $\tau = \tau^*$  and  $\mu = \mu^*$ . If  $\omega_0 \neq 0$ , a Hopf bifurcation may occur, and the GHBT establishes sufficient conditions for the appearance of a periodic solution branch related to this stability change of  $Y^*$ . The basic scheme allows an approximation of the periodic solution with two harmonics. To build the approximate expression, one needs to obtain both amplitude and frequency estimates. They can be found from the intersection between the loci of the characteristic function  $(\lambda)$  and the one associated with  $-1 + \xi_1 \theta^2$  in the complex plane, i.e., the method has a graphical interpretation. Here,  $\xi_1 \in \mathbb{C}$ is an auxiliary quantity that will be defined in short and  $\theta \in \mathbb{R}^+$  is a measure of the amplitude of the sought periodic solution. In other words, one needs to solve

$$\widehat{\lambda}(i\omega) = -1 + \xi_1(\omega)\theta^2, \tag{7}$$

for  $\theta$  and  $\omega$ , where the quantity  $\xi_1$  is given by

$$\xi_1(\omega) = -\frac{u^T G^*(i\omega) p_1(i\omega)}{u^T v}, \tag{8}$$

being u and v the left and right eigenvectors, respectively, of matrix  $G^*(i\omega)J$  associated with the eigenvalue  $\widehat{\lambda}(i\omega)$ , and

$$p_1(i\omega) = D_2 v \otimes V_{02} + \frac{1}{2} D_2 \bar{v} \otimes V_{22} + \frac{1}{8} D_3 v \otimes v \otimes \bar{v},$$
(9)

where  $(\overline{\cdot})$  represents the complex-conjugate and  $\otimes$  is the tensor product operator. Also

$$D_2 = \frac{\partial^2 g}{\partial Y^2}\Big|_{Y=Y^*}, \quad D_3 = \frac{\partial^3 g}{\partial Y^3}\Big|_{Y=Y^*},$$

are the (matrix) high-order derivatives of g and

$$V_{02} = -\frac{1}{4}H^*(0)D_2v \otimes \bar{v}, \quad V_{22} = -\frac{1}{4}H^*(2i\omega)D_2v \otimes v,$$
(10)

are the zeroth and second-order harmonics of the Fourier representation, with  $H^*(s) = [I_{2m} + G^*(s)J]^{-1}G^*(s)$  being the closed-loop transfer function of the linearized system. Finally, the second-order approximation of the periodic solution reads

$$y(t) \simeq \operatorname{Re} \left\{ \sum_{k=0}^{2} \mathcal{Y}^{k} \exp(ik\omega t) \right\},$$

where  $\mathcal{Y}^0 = \theta^2 V_{02}$ ,  $\mathcal{Y}^1 = \theta v$ ,  $\mathcal{Y}^2 = \theta^2 V_{22}$ , being  $\theta$  and  $\omega$  the solution pair of (7).

In addition, more accurate approximations, that include more harmonics can be built up [Moiola & Chen, 1996], which are usually compared with the results given by the package Dde-Biftool [Engelborghs et al., 2001]. It is important to point out that the GHBT has local validity, i.e., the obtained results become less accurate as long as the parameter value departs from the critical bifurcation value, worsening the predicted results. Moreover, the GHBT provides an expression for the first curvature coefficient (also know as the first Lyapunov focal value)  $\sigma_1$  of the emerging cycle

$$\sigma_1 = -\text{Re}\left(\frac{u^T G^*(i\omega_0) p_1(i\omega_0)}{u^T G^{*\prime}(i\omega_0) J v}\right), \qquad (11)$$

where  $G^{*\prime}(i\omega_0) = dG^*/ds|_{s=i\omega_0}$ . If  $\sigma_1$  is negative (positive), then the orbit is stable (unstable).

In two of the examples analyzed in this article, systems of the form (1) that can be represented as (5a-5c) with p=m=1, (called SISO: single input - single output) will be considered. In this simplified setting, some expressions become simpler than in the general case. For example, the use of the augmented transfer function  $G^*(s)$  is not needed, the loop gain is simply G(s)J that become scalar, the eigenvectors of G(s)J are u=v=1, and (8) reduces to

$$\xi_1(i\omega) = -G(i\omega) \left\{ D_2(V_{02} + \frac{1}{2}V_{22}) + \frac{1}{8}D_3 \right\},$$
 (12) where  $G(s)$  is given by (6) and now results

$$\sigma_1 = \operatorname{Re}\left(\frac{\xi_1(i\omega_0)}{G'(i\omega_0)J}\right).$$
 (13)

# 4. Stability and bifurcations of limit-cycles

Once that the appearance of a limit cycle  $\tilde{x}(t)$  in (1) via a Hopf bifurcation is determined, its stability is given by (11) in the most general case. However, this information is limited since it provides the stability at the birth of the cycle, but it may change as the periodic solution grows in amplitude when the parameter keeps varying. Thus, as long as the parameter values depart from the critical one, the stability of  $\tilde{x}(t)$  of principal period T can still be studied from (2). In order to solve this equation with initial data  $x(t) = \varphi(t), t \in [-\tau, 0]$  and analyze the stability of  $\tilde{x}(t)$ , the monodromy operator U, should be obtained. Under the considered hypothesis, result that U is compact, its spectrum  $\sigma(U)$  has the origin as an accumulation point and also  $1 \in \sigma(U)$ . The spectrum of U is conformed by the Floquet multipliers of the periodic solution, and the one placed at point 1 is called the trivial multiplier  $\mu_0$  [Diekmann et al., 1995]. Since in practice, it is not possible to obtain the analytical expression of U, an approximant "monodromy" matrix U (which shares the main stability properties with U) will be constructed. It means that the information about the relevant Floquet multipliers of U (those closer to the unit circle) will be found directly through the eigenvalues of U. The periodic solution is unstable when at least one of these eigenvalues lies outside of the unit circle. If the cycle is stable but after a parameter variation one eigenvalue crosses the circle through the point 1 (respectively, -1) a fold (flip, respectively) bifurcation takes place. Alternatively, if a couple of complex-conjugate eigenvalues cross the circle as the parameter varies, a Neimark-Sacker bifurcation occurs, giving place to the appearance of quasi-periodic solutions. In order to obtain the mentioned matrix U, the semidiscretization method described below will be used.

### 5. The semi-discretization method

The stability properties of equilibrium points and periodic solutions of differential equations with one or more delays can be determined by the method completely detailed in [Insperger & Stépán, 2011]. Consider again (2) where  $L_0$  and  $L_1$  are  $n \times n$  continuous matrices with T-periodic coefficients in the variable t. The case in which  $L_0$  and  $L_1$  are constant matrices (but they still depend on the parameter vector  $\mu$ ) allows to study the stability of equilibrium points, as described in Section 2. By consid-

ering the variation of two scalar parameters (two components of  $\mu$ ) or one scalar parameter and the time-delay, it is possible to obtain stability charts in different planes, distinguishing regions where the equilibrium is stable or unstable.

Once that the stability chart of an equilibrium point is determined, its boundaries usually represent Hopf bifurcation curves. In order to study the stability of a limit cycle emerging from such a point in (1), its approximate expression obtained with the GHBT described in Section 3 can be employed and replaced in (2), converting  $L_0(t,\mu)$  and  $L_1(t,\mu)$  in T-periodic matrices. It is also possible to detect bifurcations of the limit cycle under some parameter variation, and hence construct secondary bifurcation curves.

In order to introduce the method in a simple setting, fixed values of the parameter vector  $\mu$  as well as the single time-delay  $\tau$  are assumed. The general formulation can be found in [Insperger & Stépán, 2011]. Suppose that  $L_1(t,\mu) =$  $M(t,\mu)D(\mu)$  where M and  $D^T$  are matrices of size  $n \times 1$ . A partition on the interval [0,T] $\bigcup_{i=0}^{p-1} [t_i, t_{i+1}]$  is taken, thus  $h = \frac{T}{p}$  is the width of any sub-interval  $I_i$  of this partition. Starting from (2) and for each  $I_i$ , the matrices  $L_0(t)$  and  $L_1(t)$  are approximated by their mean values, and the vector of delayed state variables is replaced by some expression depending on t resulting from a linear interpolation, according to a first-order scheme. First, if  $t \in I_i$  one gets

$$\dot{y}(t) = L_{0i}y(t) + M_i D \left(\beta_{i,0}y(t_{i-r}) + \beta_{i,1}y(t_{i+1-r})\right),$$
(14)

where

$$L_{0i} = \frac{1}{h} \int_{t_i}^{t_{i+1}} L_0(s) ds, \quad M_i = \frac{1}{h} \int_{t_i}^{t_{i+1}} M(s) ds$$

and r is the natural number or 0, given by  $r=\left[\frac{\tau}{h}+\frac{1}{2}\right]$  where  $[\ ]$  represents the entire part of a real number. From now on, it is noted  $y_i = y(t_i)$  for clearness. Then, in (2), one can approximate

$$y(t-\tau) \approx y(t_i + \frac{h}{2} - \tau) = \beta_{i,0}y_{i-r} + \beta_{i,1}y_{i+1-r},$$

where

$$\beta_{i,0}(t) = \frac{(i-r+1)h-(t-\tau)}{h}, \quad \beta_{i,1}(t) = \frac{(t-\tau)+(r-i)h}{h},$$

because if  $t \in I_i$ , thus  $(t - \tau) \in [t_{i-r}, t_{i+1-r}]$  and a linear interpolation between the values  $y_{i-r}$  and  $y_{i+1-r}$  is used to represent  $y(t-\tau)$ . This procedure explains (14). Thus, the solution of the discrete system with initial values  $y_i$  and  $y_{i-r}, y_{i+1-r}$  can be found analytically in  $I_i = [t_i, t_{i+1}]$  as

$$y_{i+1} = P_i y_i + R_{i,0} y_{i-r} + R_{i,1} y_{i+1-r}, (15)$$

where  $P_i = e^{L_{0i}h}$ , is the matrix exponential  $L_{0i}h$ and, assuming that  $\det(L_{0i}) \neq 0$  the following expressions are found

$$R_{i,0} = \left[\frac{1}{h} \left(J_n(L_0{}_i^{-1}(-\tau + rh - h) + L_0{}_i^{-2}) + L_0{}_i^{-1}\right]M_i,$$
(16)

$$R_{i,1} = \left[\frac{1}{h}(J_n(L_{0_i}^{-1}(\tau - rh) - L_{0_i}^{-2}) - L_{0_i}^{-1}\right]M_i,$$
(17)

where  $J_n = I_n - e^{L_{0i}h}$ . If  $\det(L_{0i}) = 0$ , then  $R_{i,0}$  and  $R_{i,1}$  are found by numeric integration. Then, (15) is written as

$$z_{i+1} = G_i z_i,$$
where  $z_i = \begin{bmatrix} y_i^{(j)} & y_{i-1} & y_{i-2} & \cdots & y_{i+1-r} & y_{i-r} \end{bmatrix}^T$  is a augmented vector of states and  $y_i^{(j)}$  represents the components of the vector  $y(t)$  in (14) and  $G_i$  is the

block matrix

$$G_{i} = \begin{bmatrix} P_{i} & 0 & \cdots & R_{i,1} & R_{i,0} \\ 1 & 0 & \cdots & 0 & 0 \\ 0 & 1 & \cdots & 0 & 0 \\ \vdots & \vdots & \ddots & \vdots & \vdots \\ 0 & 0 & \cdots & 1 & 0 \end{bmatrix} . \tag{19}$$

Since T = ph, after p iterations of (18) with initial value  $z_0$ , the monodromy map  $z_p = \mathbf{U}z_0$  is attained, where

$$\mathbf{U} = G_{p-1}G_{p-2}\cdots G_0,\tag{20}$$

is an  $(n+r) \times (n+r)$  matrix representing the monodromy operator of (14), which in turn is a finite-dimensional approximation of the infinitedimensional monodromy operator U of (2). So, if its eigenvalues lie inside of the unit circle of the complex plane, then (14) is asymptotically stable. Under certain conditions, this discretization technique preserves the asymptotic stability in retarded DDEs, as shown in [Hartung et al., 2006]. Thus, the stability charts of (14) provide approximate stability charts of the corresponding periodic system (2).

In summary, the stability charts of equilibrium points in DDEs will be found, assuming constant matrices in (2). In the other hand, the case of timeperiodic matrices emerge when the linearized equation of a nonlinear DDE about a periodic solution is computed. The asymptotic stability of the linearized equation determines the stability of the limit cycle of the corresponding nonlinear system. Moreover, if this periodic solution is the result of a Hopf bifurcation, an approximate expression can

be built via the frequency-domain approach, to obtain a system like (2). Then, its stability can be determined thanks to the semi-discretization method. By tracking the loci of the eigenvalues of the monodromy matrix (the Floquet multipliers of the cycle) as a parameter is varied, the secondary bifurcations can be detected.

# 6. Examples

# 6.1. Tesi's system with delayed control

Consider the system introduced in [Tesi et al., 1996] with a feedback term as proposed by Pyragas [1992], given by

$$\dot{x}_1 = x_2, 
\dot{x}_2 = x_3, 
\dot{x}_3 = -x_1 - 1.2x_2 + \mu x_3 + x_1^2 + k(x_1 - x_{1\tau}),$$
(21)

where  $\mu \in \mathbb{R}$  and  $x_{1\tau} = x_1(t-\tau)$ ,  $k, \tau > 0$ . The equilibrium points result with  $x_2^* = x_3^* = 0$  and  $x_1^* = 0$  or  $x_1^* = 1$ . The stability of these points is studied via the linearized equation (2) with

$$L_0 = \begin{bmatrix} 0 & 1 & 0 \\ 0 & 0 & 1 \\ -1 + k + 2x_1^* & -1.2 & \mu \end{bmatrix}, \ L_1 = \begin{bmatrix} 0 & 0 & 0 \\ 0 & 0 & 0 \\ -k & 0 & 0 \end{bmatrix},$$

given in (3), where  $x_1^* = 0$  or  $x_1^* = 1$ , depending upon the considered point.

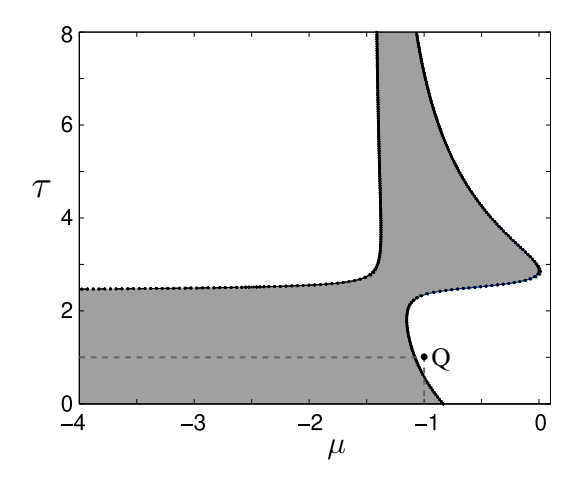


Fig. 1. Stability chart of the trivial equilibrium of system (21) in the  $(\mu,\tau)$  plane with k=0.5. This equilibrium is asymptotically stable in the shaded region. The results obtained by semi-discretization technique and those of Dde-Biftool (dots) are indistinguishable. At a particular point denoted as Q=(-1,1), a periodic solution emerging from a Hopf bifurcation will be approximated.

In this example, it is taken  $x_1^* = 0$  and the system is discretized with  $\mu = 1, k = 0.5, \tau = 1 = T$ , and p = 10. Notice that the period T can be chosen arbitrarily for the analysis of a constant solution. Then, for this particular set of parameters, one has  $h = \frac{\dot{T}}{p} = \frac{1}{10}$  and  $r = [\frac{\tau}{h} + 0.5] = 10$ . Observe that in this example  $L_1 = M.D$  where  $M^T = [0 \ 0 \ -k]$ and  $D = [1\ 0\ 0]$ . In this way, from the partition  $[0,T] = \bigcup_{i=0}^{9} [t_i, t_{i+1}], \text{ the matrix } G_i \text{ (19) results}$ of size 13 = 3 + 10, where n = 3 is the dimension of x, r = 10 and  $G_i(1:3,1:3) = \exp(L_0)$ ,  $G_i(4,1:3) = \begin{bmatrix} 1 & 0 & 0 \end{bmatrix}, G_i(5:13,4:12) = I_9,$  $G_i(1:3,12) = R_{i,1}$  and  $G_i(1:3,13) = R_{i,0}$ . Under the successive application of  $G_i$ , one can obtain U as in (20) and determine the stability charts of the equilibrium point  $(x_1^*, x_2^*, x_3^*) = (0, 0, 0)$ . For example, for a constant value of k (k = 0.5), the stability region of the trivial equilibrium point in the  $(\mu, \tau)$ parameter space can be achieved. On this regard, consider  $\mu \in [-4,0], \tau \in [0,8]$  and a grid of  $40\times40$ points to compute  $G_i$  as described in Section 5. Notice that the size of  $G_i$  also varies step by step conforming  $\tau$  varies. The obtained stability region is shown in Fig. 1, where the result agrees with the equivalent given by Dde-Biftool.

The original model [Tesi et al., 1996] which has only one real parameter and does not include any delay, exhibits a supercritical Hopf bifurcation. So it is interesting to observe the evolution of the stability charts of (21) at the equilibrium point while k tends to 0, to recover the phenomena of the original system. These results are shown in Fig. 2.

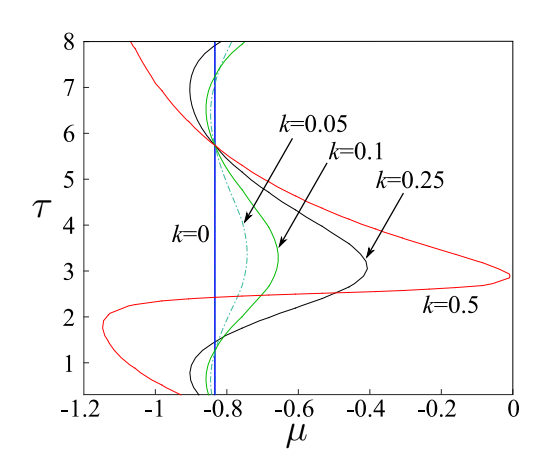


Fig. 2. Stability chart portions for the trivial equilibrium of system (21) in the  $(\mu,\tau)$  plane for several values of k. These curves approach to the line  $\mu=-\frac{5}{6}$ , as k tends to 0, which is the Hopf bifurcation condition for the original system [Tesi et al., 1996]. The one for k=0.5 corresponds to the chart shown in Fig. 1.

In order to represent (21) in the form (5a-5c), the following matrices are considered

$$A_0 = \begin{bmatrix} 0 & 1 & 0 \\ 0 & 0 & 1 \\ -1 & -1.2 & \mu \end{bmatrix}, A_1 = \begin{bmatrix} 0 & 0 & 0 \\ 0 & 0 & 0 \\ -k & 0 & 0 \end{bmatrix},$$
$$B = \begin{bmatrix} 0 & 0 & 1 \end{bmatrix}^T, C = \begin{bmatrix} 1 & 0 & 0 \end{bmatrix},$$

and  $u(t) = g(y(t)) = -ky(t) + y(t)^2$ , with  $y = -x_1$ . Matrix G representing the linear part of the system

$$G(s) = C[sI_3 - A_0 - A_1e^{-s\tau}]^{-1}B = \frac{1}{\Delta(s)},$$

where  $\Delta(s) = s^3 - \mu s^2 + 1.2s + ke^{-s\tau} + 1$ . The equilibrium points in the frequency-domain representation are given by the equation G(0)g(y) = -y, and the solutions are  $y_1^* = 0$  and  $y_1^* = -1$ . The stability of the trivial equilibrium is determined by the characteristic equation of G(s)J, where  $J = \frac{dg}{dy}\Big|_{y=0} =$  $[-k+2y]_{y=0}$ . Since it is a scalar matrix, the Hopf bifurcation condition becomes

$$G(s)J = -1 \iff s^3 - \mu s^2 + 1.2s + ke^{-s\tau} + 1 - k = 0.$$

Amplitude and frequency estimates of the orbit emerging from the Hopf bifurcation can be obtained by solving (7) with  $\lambda(i\omega) = G(i\omega)J = -k/\Delta(i\omega)$ and  $\xi$  given by (12). The Hopf bifurcation necessary condition  $\hat{\lambda}(i\omega) = -1$  reads

$$\begin{cases} \omega^2 \mu + k \cos \omega \tau + 1 - k = 0, \\ -\omega^3 + 1.2\omega - k \sin \omega \tau = 0. \end{cases}$$
 (22)

If k = 0.5 and  $\tau = 1$ , a Hopf bifurcation point results from (22) with  $\mu_0 = -1.0794$  and  $\omega_0 = 0.8724$ . Thus, one can choose the point Q = (-1, 1) shown in Fig. 1 in order to compute the stability of the periodic solution emerging from the aforementioned Hopf point. Using a second-order harmonic balance (HB2), the approximate expression of the  $x_1$  component of this cycle results

$$x_1 = 0.0380 - 0.2757\cos(\omega t) -0.0048\cos(2\omega t) - 0.0068\sin(2\omega t),$$

where  $\omega = 0.8666$ . Analogously, the fourth (HB4) and sixth (HB6) order approximations can be obtained following the formulae in [Gentile et al., 2019. With these results, the semi-discretization method is applied to determine the stability of the periodic solution, via an approximation of the monodromy operator given by (20). The results are shown in Table 1, where the trivial multiplier  $\mu_0$ and the following (of greater modulus) multiplier

 $\mu_1$  are compared. In one case they are computed via different harmonic balances and in the other with Dde-Biftool [Engelborghs et al., 2001]. The obtained values confirm the existence of an asymptotically stable cycle, and the accuracy of the approximations improves conforming a higher-order balance is employed, approaching the values given by Dde-Biftool. Another measure of the accuracy of the approximation is the closeness of the trivial multiplier  $\mu_0$  to the point 1.

Table 1. Stability analysis of the cycle in model (21) with  $k = 0.5, (\mu, \tau) = (-1, 1)$  (point Q in Fig. 1) via semi-discretization, with different harmonic balances and comparisons with Dde-Biftool.

	$\theta$	$\omega$	$\mu_0$	$\mu_1$
HB2	0.2757	0.8666	1.0101	0.7881
HB4	0.2721	0.8669	1.0084	0.7951
HB6	0.2718	0.8669	1.0084	0.7955
Dde-Biftool	0.2705	0.8677	1.0000	0.8049

#### 6.2. System of Campbell and Leblanc

The following model, introduced in [Campbell & LeBlanc, 1998] is considered

$$\ddot{x} + \alpha \dot{x} + \frac{5}{2}x = ax_{\tau} + bx_{\tau}^{2}, \tag{23}$$

where  $\alpha, a, b$  are parameters,  $x_{\tau} = x(t - \tau)$  and  $\tau > 0$ . Equation (23) can be written as

$$\dot{x}_1 = -\alpha x_1 - \frac{5}{2}x_2 + ax_{2\tau} + bx_{2\tau}^2, 
\dot{x}_2 = x_1.$$
(24)

The equilibrium points result with  $x_1^* = 0$  and  $x_2^*$ being the solution of  $-\frac{5}{2}x_2 + ax_2 + bx_2^2 = 0$ , thus  $x_2^* = 0$  or  $x_2^* = (\frac{5}{2} - a)b^{-1}$ . The dynamics close to the trivial equilibrium with  $\alpha = 0$  was analyzed in [Itovich et al., 2019] considering the variation of the main parameters a and  $\tau$ . The regions of asymptotic stability were determined in several parameter planes by studying the exponential polynomial characteristic equation. Moreover, the appearance of periodic solutions was found via the GHBT as well as the suspection of fold bifurcations of cycles, the latter confirmed using Dde-Biftool. Now, taking into account the results in [Campbell & LeBlanc, 1998], it is known that a Hopf-Hopf (HH) bifurcation with 1:2 resonance appears with  $\alpha = 0$ , at  $(\tau, a) = (k\pi, -3/2), k \in \mathbb{N}$ . Now consider k = 1 and let  $\tau$  and a vary. The stability of the trivial equilibrium  $x^* = (x_1^*, x_2^*) = (0, 0)$  of (24) is determined by

the linear delay equation (2), where

$$L_0 = \begin{bmatrix} 0 & -\frac{5}{2} \\ 1 & 0 \end{bmatrix}, \ L_1 = \begin{bmatrix} 0 & a \\ 0 & 0 \end{bmatrix},$$

according with the location of the roots of  $P(\lambda) = \det(\lambda I - L_0 - L_1 e^{-\lambda \tau}) = \lambda^2 + \frac{5}{2} - a e^{-\lambda \tau}$ . It is useful to depict the stability chart in the  $(\tau, a)$  plane, which is obtained via the semi-discretization method, detecting the curves where the equilibrium changes its stability, and testing arbitrary points of the resulting regions. The result can be seen in Fig. 3.

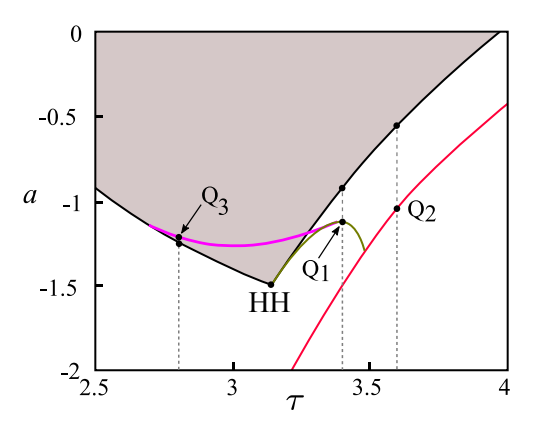


Fig. 3. Stability chart delimited by some portions of Hopf bifurcation curves for system (23), close to a Hopf-Hopf with 1:2 resonance point (HH) appearing for  $\alpha=0$  at  $(\tau,a)=(\pi,-3/2)$ . The shaded region indicates asymptotic stability. By previous knowledge (see Gentile *et al.*, 2018) of the existence of flip, Neimark-Sacker and fold bifurcation curves (displayed in green, red and pink, respectively) some secondary bifurcations are detected at the points labeled as  $Q_1, Q_2$  and  $Q_3$ .

It is also possible to apply the frequencydomain approach to (24) in order to find periodic solutions emanating from Hopf bifurcations. In this sense (see Gentile et al., 2018), the case b = 0.9was considered for system (23) and the dynamics around the HH bifurcation with 1:2 resonance point  $(\alpha = 0, \tau = \pi, a = -3/2)$  was studied in detail using the Dde-Biftool. Moreover, the existence of fold, flip and Neimark-Sacker secondary bifurcations was proved numerically. These bifurcations can be also recovered with the combined techniques described in this work. The approximate expressions of the periodic solutions emerging from Hopf bifurcations are obtained via the GHBT, and their stability is determined as described in Example 6.1 in this section. It is clear that the quasianalytic formulae of the cycle changes as one selected system parameter varies.

For example, in Fig. 3, three vertical dotted lines are shown, assuming fixed values of  $\tau$  and allowing a to vary. In each case, the expressions of the emerging cycles are constructed via the GHBT and continued as functions of the parameter a. The Floquet multipliers of the approximant matrix are computed step by step, so this mechanism allows to follow their evolution. Thus, the cycle bifurcations mentioned above can be detected again and checked, as shown in Tables 2-4, where the information about the trivial multiplier and the amplitude of the cycle is also given. These determinations are shown in Fig. 3 labeled as  $Q_1$ ,  $Q_2$  and  $Q_3$ , together with some related cycle bifurcations curves obtained previously in [Gentile et al., 2018]. It is well known that the singularity caused by the vanishing of the first curvature coefficient (13) causes the appearance of fold bifurcations of cycles. As example, to find a point where a fold appears, fourth-order approximations were used (by technical reasons, the second-order expressions cannot be used for this specific task) together with the semi-discretization method. These results, which involve the point  $Q_3$ located in Fig. 3, can be seen in Table 4 and are in agreement with those obtained in [Gentile et al., 2018]. This singularity is very close to some initial Hopf point pointed out in Table 4 and at least two reasons can justify this particular determination: the branch of periodic solutions grows in amplitude very quickly and the GHBT can guarantee results only when  $\theta \leq 1$ .

Table 2. Determination of a flip bifurcation point  $Q_1$  with  $\tau = 3.4$  near to the Hopf point  $(\tau, a) = (3.4, -0.9151)$  with  $w_0 = 1.8480$  for system (23)

$\omega_0 = 1.0400$ , for system (23).				
	a	$\mu_0$	$\theta$	
HB2	-1.1130	0.9969	1.0375	
HB4	-1.1206	0.9999	1.0337	
Dde-Biftool	-1.1235	1	1.0549	

Table 3. Determination of a Neimark-Sacker bifurcation point Q<sub>2</sub> with  $\tau=3.6$  near to the Hopf point  $(\tau,a)=(3.6,-0.5462)$  with  $\omega_0=1.7453$ , for system (23).

	a	$\mu_0$	$\theta$
HB2	-0.9830	0.9867	1.5324
HB4	-1.0330	1.0085	1.5405
Dde-Biftool	-1.0352	1	1.5430

Table 4: Determination of a fold bifurcation point Q<sub>3</sub> with  $\tau = 2.8$  near to the Hopf point  $(\tau, a) = (2.8, -1.2411)$  with

$\omega_0 = 1.1220$ , for system (23).				
	a	$\mu_0$	$\theta$	
HB4	-1.2226	0.9980	0.6386	
Dde-Biftool	-1.2211	1	0.6459	

#### Van der Pol system with 6.3. time-delay

It is considered the modified delayed van der Pol system studied in [Gentile et al., 2019], given by

$$\ddot{x} + (x^2 - \varepsilon)x_\tau + x = 0, \tag{25}$$

with  $\varepsilon > 0$ , which can be rewritten as

$$\begin{cases} \dot{x}_1 = -(x_2^2 - \varepsilon)x_{2\tau} - x_2, \\ \dot{x}_2 = x_1, \end{cases}$$
 (26)

after defining the state variables  $x_2 = x$  and  $x_1 = \dot{x}$ . System (26) has three equilibrium points with  $x_1^* =$ 0 and  $x_2^* = 0$  or  $x_2^* = \pm \sqrt{\varepsilon - 1}$ , when  $\varepsilon > 1$ . Following (3), the linearization about any equilibrium point results:

$$L_0 = \begin{bmatrix} 0 & -1 - 2(x_2^*)^2 \\ 1 & 0 \end{bmatrix}, \ L_1 = \begin{bmatrix} 0 & \varepsilon \\ 0 & 0 \end{bmatrix}, \quad (27)$$

where  $x_2^*$  assumes the value in accordance with the considered equilibrium point. Then, some aspects related with stability of equilibrium points and orbits coming from Hopf bifurcations will be considered.

#### 6.3.1. About its equilibrium points

The stability charts for the equilibrium points are build following the strategy shown in the previous examples. For the case of the trivial equilibrium, with  $x_2^* = 0$ , (see (27)) the chart is obtained through semi-discretization and shown in Fig. 4. This representation is similar to one found before in [Itovich et al., 2019. Besides, one theorem can be stated to establish stability areas exactly, due to the border curves can be obtained as exact formulas (see Itovich *et al.*, 2019).

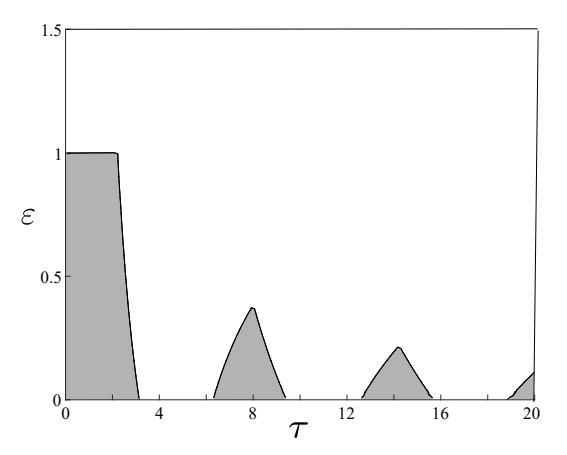


Fig. 4. Stability chart for the trivial equilibrium point for system (25). The borders of the shadowed regions represent Hopf bifurcation curves.

Moreover, for any of remaining two equilibrium points with  $x_2^* = \pm \sqrt{\varepsilon - 1}$ , the semi-discretization method yields a stability chart that looks more complex than the previous and is exhibited in Fig. 5.

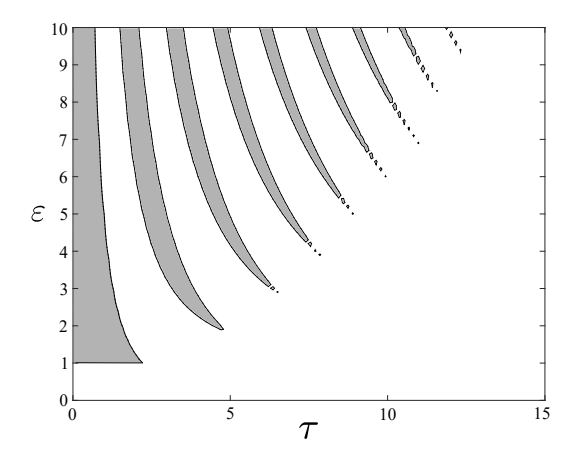


Fig. 5. Stability chart for the non trivial equilibrium points for system (25). The frontiers of these tongues are defined by the collection of curves  $(\tau, \varepsilon)$  in the condition (28).

Furthermore, it is possible to confirm the asymptotic stability areas analytically, employing Pontryagin results [Bellman & Cooke, 1963] with an analogous strategy as in [Itovich et al., 2019] through the new following outcome:

Theorem: Suppose that  $\varepsilon > 1$  in (25) or system (26). The sufficient and necessary condition that the parameters  $(\tau, \varepsilon)$  must satisfy to have the asymptotic stability at any of the non trivial equilibrium points is given by the general condition

$$\frac{(2k)^2\pi^2}{2\tau^2} + 1 < \varepsilon < \frac{(2k+1)^2\pi^2}{2\tau^2} \tag{28}$$

where k = 0 or  $k \in \mathbb{N}$ .

# 6.3.2. About its periodic solutions

System (26) can also be represented in a feedback form considering

$$G^*(s) = \frac{1}{s^2} [1 \ e^{-s\tau}]^T \qquad g(Y) = (y^2 - \varepsilon)y_\tau + y,$$

where  $Y=[y \ y_{\tau}]$ . Thus with the frequency domain approach, for the trivial equilibrium  $Y^*=(y^*,y^*_{\tau})=(0,0)$ , the Jacobian matrix is  $J=[1-\varepsilon]$ . Since rank  $G^*(s)J=1$ , its only nonzero eigenvalue is given by  $\widehat{\lambda}(s)=(1-\varepsilon e^{-s\tau})/s^2$ , for which the necessary Hopf bifurcation condition  $(\widehat{\lambda}(i\omega_0)=-1)$  reads

$$\begin{cases} \varepsilon \cos(\omega_0 \tau) = 1 - \omega_0^2, \\ \varepsilon \sin(\omega_0 \tau) = 0. \end{cases}$$

There is a trivial solution given by  $\omega_0=1$  and  $\varepsilon=0$ , the same appearing for the non-delayed system. On the other hand, there is a set of solutions with  $\omega\tau=n\pi,\ n\in\mathbb{N}\cup\{0\}$  that result in  $\varepsilon(-1)^n=1-(n\pi/\tau)^2$  after replacing into the first equation. Thus, the Hopf curves in the  $(\tau,\varepsilon)$  plane can be obtained also from the last expression and are in agreement with (28), limiting the stability regions in Fig. 5.

Since the output of the linear subsystem is non-scalar, the general expression for the curvature coefficient (11) is used. After some calculations, for the solution  $\omega_0=1$  and  $\varepsilon=0$ , follows  $\sigma_1=\sin(\tau)/8$ , then the bifurcation is supercritical if  $\sin\tau<0$  and subcritical if  $\sin\tau>0$ . This information agrees with the results shown in Tables 5 and 6, for two particular choices of the parameters  $(\tau,\varepsilon)$ , given a stable or an unstable cycle, respectively. From the second equation the amplitude is given by  $\theta=2\varepsilon^{1/2}$ , thus  $\max(x(t))=2\varepsilon^{1/2}$ .

Since the matrix representing the second-order derivative in (9) is zero for the trivial equilibrium, it is not difficult to develop up to fourth-order harmonic balance. Taking into account the procedure given in [Moiola & Chen, 1996; Gentile et al., 2019], one can obtain the following expressions for the harmonics

$$\begin{split} &\mathcal{Y}^0 = \mathbf{0}, \quad \mathcal{Y}^1 = 2\sqrt{\varepsilon} \begin{bmatrix} 1 \\ e^{-i\omega\tau} \end{bmatrix}, \quad \mathcal{Y}^2 = \mathbf{0}, \\ &\mathcal{Y}^3 = -\frac{2\varepsilon^{3/2}}{\psi(\omega)} \begin{bmatrix} e^{-i\omega\tau} \\ e^{-i4\omega\tau} \end{bmatrix}, \quad \mathcal{Y}^4 = \mathbf{0}, \end{split}$$

where  $\psi(\omega) = 1 - 9\omega^2 - \varepsilon e^{-i3\omega\tau}$  and  $\omega$  is obtained by solving

$$\widehat{\lambda}(i\omega) = -1 + \xi_1 \theta^2 + \xi_2 \theta^4, \tag{29}$$

with

$$\xi_1 = (\frac{1}{2}e^{-i\omega\tau} + \frac{1}{4}e^{i\omega\tau})/\omega^2,$$
  

$$\xi_2 = -(2 + e^{-i4\omega\tau})/(16\omega^2\psi(\omega)).$$

Particularly, for the second order harmonic balance, the frequency  $\omega$  follows from (29) considering  $\xi_2 = 0$  and the expression for the cycle results just with  $\mathcal{Y}^1$ . To apply the semi-discretization method one needs the expression of the periodic solution to replace it in (27) and then one follows the steps described in Section 5.

In order to test the stability of the cycles emerging from Hopf bifurcations curves (see Fig. 4), a pair of representative examples have been considered and the outcomes can be observed in Tables 5 and 6.

Table 5. Stability analysis of the stable cycle in model (26) with  $\tau=4$ , and  $\varepsilon=0.05$  via semi-discretization, with different harmonic balances and comparison with

	$\theta$	$rac{ ext{ftool result}}{\omega}$	$\mu_0$	$\mu_1$
HB2	0.4472	0.9611	1.0292	0.7688
HB4	0.4480	0.9611	0.9954	0.7959
Dde-Biftool	0.4451	0.9610	1.0000	0.7923

Table 6. Stability analysis of the unstable cycle in model (26) with  $\tau=1$ , and  $\varepsilon=0.05$  via semi-discretization, with different harmonic balances and comparison with

Dde-Biftool results.				
	heta	$\omega$	$\mu_0$	$\mu_1$
HB2	0.4472	1.0256	1.0075	1.2648
HB4	0.4485	1.026	1.0011	1.2761
Dde-Biftool	0.4495	1.026	1.0000	1.2780

## 7. Conclusions

In this work, the usefulness of the combination between the GHBT and the semi-discretization techniques, to study stability and bifurcations in delayed equations, is demonstrated. This hybrid method allows to determine the stability regions of equilibrium points, the stability of limit cycles emerging from Hopf bifurcations and to detect secondary bifurcations. Moreover, stability charts with the identification of those secondary bifurcations

were built. The accuracy on the detection of those global phenomena relies on the proximity between the secondary bifurcation point and the initial Hopf bifurcation point that gives birth to the limit cycle, as well as on the order of the harmonic balance employed. The obtained results successfully agree with those given by the software Dde-Biftool. In future contributions, the goal is to use this hybrid technique to study the dynamics around more complex singularities, and also to analyze delay equations of neutral type.

# Acknowledgments

The authors acknowledge the founding provided by Universidad Nacional de Río Negro (PI 40/A1076), Universidad Nacional del Sur (PGI 24/K087) and CONICET (PIP 11220200102076).

#### References

- Balanov, A., Janson, G. N. B. & Schöll, E. [2005] "Delayed feedback control of chaos: Bifurcation analysis," Physical Review E 71, 016222.
- Bellman, R. & Cooke, K. [1963] Differential-Difference Equations, Academic Press, New York.
- Butcher, E. & Mann, B. [2009] "Stability analysis and control of linear periodic delayed systems using Chebyshev and temporal finite element methods," in B. Balachandran et al. (eds.), Delay Differential Equations: Recent Advances and New Directions, Springer Series, pp. 93-129.
- Campbell, S. A. & LeBlanc, V. G. [1998] "Resonant Hopf-Hopf interactions in delay differential equations," J. Dyn. Differ. Equations **10**(2), pp. 327–346.
- Diekmann, O., van Gils, S. A., Verduyn Lunel, S. M. & Walther, H. [1995] Delay Equations, Applied Mathematical Sciences Vol. 110, Springer, New York.
- Engelborghs, K., Luzyanina, T. & Samaey, G. [2001] "DDE-BIFTOOL v.2.00: A Matlab package for bifurcation analysis of delay differential equations," Tech. Report 330, Department of Computer Science, K.U. Leuven, Belgium.
- Gentile F. S., Itovich, G. R. & Moiola J. L. [2018] "Resonant 1:2 double Hopf bifurcation in an

- oscillator with delayed feedback," Nonlinear Dyn. **91**(3), pp. 1779–1789.
- Gentile, F. S., Moiola J. L. & Chen, G. R. [2019] Frequency-Domain Approach to Hopf Bifurcation Analysis: Continuous Time-delay Systems, World Scientific, Singapore.
- Hartung, F., Insperger, T., Stépán, G. & Turi, J. [2006] "Approximate stability charts for milling processes using semi-discretization," App. Math. and Computations 174, pp. 51-73.
- Insperger, T. & Stépán, G. [2011] Semi-Discretization for Time-Delay Systems: Stability and Engineering Applications, Springer Science+Business Media, Applied Mathematical Sciences Vol. 178.
- Itovich, G. R., Gentile, F. S. & Moiola, J. L. [2019] "Hybrid methods for studying stability and bifurcations in delayed feedback systems," Int. J. of Bifurc. and Chaos 29, 12, 1950167 1-15.
- Kharitonov, V. L., Niculescu, S. I., Moreno J. & Michiels, W. [2005] "Static output feedback stabilization: Necessary conditions for multiple delay controllers," IEEE Trans. on Automatic Control 50(1), pp. 82-86.
- Mees, A. I. [1981] Dynamics of Feedback Systems, John Wiley & Sons, Chichester, UK.
- Mees, A. I. & Chua, L. O. [1979] "The Hopf bifurcation theorem and its applications to nonlinear oscillations in circuits and systems," IEEE Trans. Circuits Syst. 26(4), pp. 235–254.
- Moiola, J. L. & Chen, G. [1996] Hopf Bifurcation Analysis: A Frequency-Domain Approach, Vol. 21, World Scientific, Singapore.
- Nakajima, H. [1997] "On analytical properties of delayed feedback control of chaos," Physics Letters, Sect. A: General, Atomic and Solid State Physics 232(3-4), pp. 207-210.
- Pyragas, K. [1992] "Continuous control of chaos by self-controlling feedback," Physics Letters A 170(6), pp. 421–428.
- Tesi, A., Abed, E. H., Genesio, R. & Wang, H. O. [1996] "Harmonic balance analysis of perioddoubling bifurcations with implications for control of nonlinear dynamics," Automatica 32, pp. 1255-1271.
- Tsypkin, Ya. Z. [1946] "Stability of systems with delayed feedback," Automat. Telemekh. 7, pp. 107–129 (also in MacFarlane, A. G. J. (ed.) [1979] Frequency-Response Methods in Control Systems, IEEE Press, pp. 45-56).